SHEAR BUCKLING OF CHANNEL SECTIONS WITH SIMPLY SUPPORTED ENDS USING THE SEMI-ANALYTICAL FINITE STRIP METHOD

CAO HUNG PHAM
GREGORY J. HANCOCK

RESEARCH REPORT R931
FEBRUARY 2013

ISSN 1833-2781

SCHOOL OF CIVIL ENGINEERING

THE UNIVERSITY OF SYDNEY

THE UNIVERSITY OF SYDNEY

SCHOOL OF CIVIL ENGINEERING

SHEAR BUCKLING OF CHANNEL SECTIONS WITH SIMPLY SUPPORTED ENDS USING THE SEMI-ANALYTICAL FINITE STRIP METHOD

RESEARCH REPORT R931

GREGORY J. HANCOCK
CAO HUNG PHAM

February 2013

ISSN 1833-2781

School of Civil Engineering, Research Report R931

Shear Buckling of Channel Sections with Simply Supported Ends
using the Semi-Analytical Finite Strip Method

Gregory J. Hancock
Cao Hung Pham

February 2013

ISSN 1833-2781

Published by:
School of Civil Engineering
The University of Sydney
Sydney NSW 2006
Australia

This report and other Research Reports published by the School of Civil Engineering are available at http://sydney.edu.au/civil

ABSTRACT

Buckling of thin-walled sections in pure shear has been recently investigated using the Semi-Analytical Finite Strip Method (SAFSM) to develop the "signature curve" for sections in shear. The method assumes that the buckle is part of an infinitely long section unrestrained against distortion at its ends. For sections restrained at finite lengths by transverse stiffeners or other similar constraints, the Spline Finite Strip Method (SFSM) has been used to determine the elastic buckling loads in pure shear. These loads are higher than those from the SAFSM due to the constraints.

The SFSM requires considerable computation to achieve the buckling loads due to the large numbers of degrees of freedom of the system. In the 1980's, Anderson and Williams developed a shear buckling analysis for sections in shear where the ends are simply supported based on the exact finite strip method. The current report further develops the SAFSM buckling theory of YK Cheung for sections in pure shear accounting for simply supported ends using the methodology of Anderson and Williams. The theory is applied to the buckling of plates of increasing length and channel sections in pure shear also for increasing length. The method requires increasing numbers of series terms as the sections become longer. Convergence studies with strip subdivision and number of series terms is provided in the report.

KEYWORDS

Cold-formed channel sections; Simply supported ends; Shear buckling analysis; Finite strip method; Semi-analytical finite strip method; Complex mathematics.

TABLE OF CONTENTS

INTRODUCTION

The recent development of the Direct Strength Method (DSM) of design, as specified in the North American Specification NAS S100 (AISI, 2007) for the design of cold-formed steel structural members and the Australian/New Zealand Standard AS/NZS 4600:2005 (Standards Australia, 2005), has required the need to compute the local, distortional and overall elastic buckling loads of full sections. The usual approach is to compute the buckling signature curves for the sections using a finite strip buckling analysis method such as in the programs CUFSM (Adany and Schafer, 2006) and THIN-WALL (CASE, 2006).

A recent development has been the DSM for sections in pure shear (Pham and Hancock, 2012a) as currently balloted for acceptance in the 2012 Edition of the NAS S100. The method requires the elastic buckling load of full sections in pure shear to be computed. The complex semi-analytical finite strip method (SAFSM) of Plank and Wittrick (1974) has been used by Hancock and Pham (2011, 2012) to compute the signature curves for channel sections in pure shear. The method assumes the ends of the half-wavelength under consideration are free to distort and the buckle is part of a very long length without restraint from end conditions. Detailed studies of sections with rectangular and triangular intermediate stiffeners in the web have been performed by Pham SH, Pham CH and Hancock (2012a, 2012b) using this analysis.

In practice, sections may be restrained at their ends or by transverse stiffeners so that the shear buckling modes are changed and the buckling loads increased by the end effects. Pham and Hancock (2009a, 2012b) have used the Spline Finite Strip Method (SFSM) developed for elastic buckling by Lau and Hancock (1986) to study channel sections with simply supported ends in shear. Although it is much more efficient than the Finite Element Method (FEM), it still requires substantial computer resources to obtain a result. Anderson and Williams (1985) have proposed a version of the exact finite strip buckling analysis developed by Wittrick (1968), and Williams and Wittrick (1969), accounting for simply supported end conditions for sections in shear. This report further develops and evaluates this method for the SAFSM of Plank and Wittrick (1974). Comparisons with the SFSM are provided to establish the accuracy.

THEORY

STRIP AXES AND NODAL LINE DEFORMATIONS

The x-axis is in the longitudinal direction in the plane of the strip, the y-axis is in the transverse direction in the plane of the strip, and w is in the z-direction perpendicular to the strip as shown in Fig. 1.

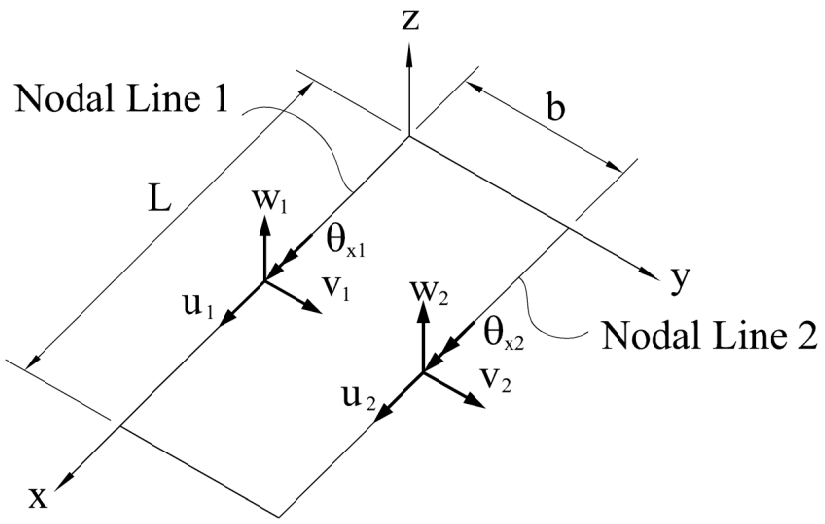

Figure 1. Strip Axes and Nodal Line Deformations

The strip nodal line flexural deformations in Fig. 1 are given in vector format by:

$$\{\delta_F\} = (w_1, \theta_{x1}, w_2, \theta_{x2})^T \quad (1)$$

Similarly, the strip nodal line membrane deformations in Fig. 1 are given in vector format by:

$$\{\delta_M\} = (u_1, v_1, u_2, v_2)^T \quad (2)$$

In the finite strip method of Cheung (1968, 1976), longitudinal variations of displacement are described by harmonic functions and transverse variations are described by polynomial functions.

PLATE BUCKLING DEFORMATIONS WITH SIMPLY SUPPORTED ENDS

For the analysis of plates and sections with simply supported ends, the strip nodal line deformations are regrouped into those associated with variation according to the sine function, and those associated with variation according to the cosine function as $\{\delta_s\} = (v_1, w_1, \theta_{x1}, v_2, w_2, \theta_{x2})^T$ and $\{\delta_c\} = (u_1, u_2)^T$ respectively. The deformations $\{\delta\}$ of a strip for μ series terms assuming simply supported ends can therefore be expressed by:

$$\{\delta\} = \mathrm{Re} \sum_{m=1}^{\mu} \begin{bmatrix} i\{\delta_s\} \\ \{\delta_c\} \end{bmatrix}_m X_1(x) = \sum_{m=1}^{\mu} \begin{bmatrix} -\{\delta_{sm}\} \sin\left(\frac{m\pi x}{L}\right) \\ \{\delta_{cm}\} \cos\left(\frac{m\pi x}{L}\right) \end{bmatrix} \quad (3)$$

where $\{\delta_{sm}\}^T = (v_1, w_1, \theta_{x1}, v_2, w_2, \theta_{x2})_m{}^T$ and $\{\delta_{cm}\}^T = (u_1, u_2)_m{}^T$

and

$$X_1(x) = \cos\left(\frac{m\pi x}{L}\right) + i \sin\left(\frac{m\pi x}{L}\right) \quad (4)$$

The symbol *Re* means the "real part", m is the number of the series term, and the elements of $\{\delta_{sm}\}$ and $\{\delta_{cm}\}$ are real. The displacements in Equation 3 satisfy the simply supported boundary conditions.

FORCES ALONG THE NODAL LINES

There are N nodal lines corresponding to the intersection of strips both at plate junctions and within plates subdivided into strips. The forces at the nodal lines can be computed at a given load factor λ_E from the unrestrained stiffness and stability matrices for the mth series term derived in Hancock and Pham (2011 2012) using:

$$\{F_m\} = [H_m]\{\delta_m\} \quad (5)$$

where $[H_m] = [K_m] - \lambda_E [G_m]$

The stiffness matrix $[K_m]$ is real and the stability matrix $[G_m]$ is real when the shear stresses shown in Fig. 2 are zero but complex Hermitian when the shear stresses are non-zero. The load factor λ_E applies to the stresses shown for each strip as in Fig. 2.

Equation 5 for the nth series term can be partitioned according to the sequence in Equation 3 so that:

$$\begin{bmatrix} \{F_s\} \\ i\{F_c\} \end{bmatrix}_n = \begin{vmatrix} [H_{11}] & [H_{12}] \\ [H_{21}] & [H_{22}] \end{vmatrix}_n \begin{bmatrix} i\{\delta_s\} \\ i\{\delta_c\} \end{bmatrix}_n \quad (6)$$

The forces are out-of-phase with the displacements so that the multiple i on $\{F_c\}$ and $\{\delta_c\}$ accounts for the 90 degree phase difference between these two components when the shear is zero, so that $[H_n]$ is real and symmetric for such cases.

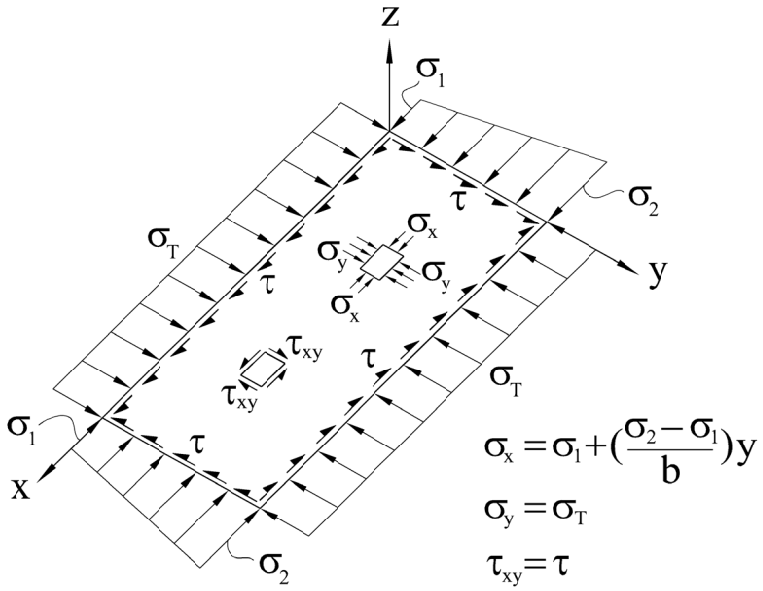

Figure 2. Membrane Stresses

The forces along the nodal lines corresponding to the assumed displacements in Equation 3 are derived as follows:

$$\{F\} = \mathrm{Re}\ \sum_{n=1}^{\mu} \begin{bmatrix} \{F_s\} \\ \{F_c\} \end{bmatrix}_n X_1(x)$$

$$= \sum_{n=1}^{\mu} \begin{bmatrix} -([H_{11}^R]\{\delta_s\} + [H_{12}^R]\{\delta_c\})_n \sin\left(\frac{n\pi x}{L}\right) - ([H_{11}^I]\{\delta_s\} + [H_{12}^I]\{\delta_c\})_n \cos\left(\frac{n\pi x}{L}\right) \\ ([H_{21}^R]\{\delta_s\} + [H_{21}^R]\{\delta_c\})_n \cos\left(\frac{n\pi x}{L}\right) - ([H_{21}^I]\{\delta_s\} + [H_{22}^I]\{\delta_c\})_n \sin\left(\frac{n\pi x}{L}\right) \end{bmatrix} \quad (7)$$

where superscripts *R* and *I* denote real and imaginary parts respectively.

TOTAL ENERGY

In order to compute the stiffness and stability matrices of the strip according to conventional finite strip theory (Cheung 1968, 1976) and buckling theory (Plank and Wittrick (1974)), it is necessary to determine the total energy in the strip under the action of the membrane forces.

The total energy *E* is given by:

$$E = \frac{1}{2}\int_0^L \{\delta\}^T\{F\}\ dx = \frac{L}{4}\sum_{m=1}^{\mu}\{\delta_m\}^T[H_m^R]\{\delta_m\}$$

$$+ \frac{L}{2}\sum_{m=1}^{\mu}\sum_{n=1}^{\mu}(c_{mn}\{\delta_{sm}\}^T([H_{11}^I]\{\delta_s\} + [H_{12}^I]\{\delta_c\})_n - c_{nm}\{\delta_{cm}\}^T([H_{21}^I]\{\delta_s\} + [H_{22}^I]\{\delta_c\})_n) \quad (8)$$

where $\{\delta_m\}^T = [\{\delta_{sm}\}^T \quad \{\delta_{cm}\}^T]$

and $$c_{mn} = \frac{1}{L}\int_0^L \sin\left(\frac{m\pi x}{L}\right)\cos\left(\frac{n\pi x}{L}\right)dx \quad (9)$$

$$= \frac{2m}{\pi(m^2 - n^2)} \quad m+n \text{ odd}$$

$$= 0 \quad m+n \text{ even}$$

STIFFNESS AND STABILITY MATRICES

For equilibrium, the theorem of minimum total potential energy with respect to each of the elements $\{\delta_m\}$ is:

$$\frac{\partial E}{\partial\{\delta_m\}} = 0 \tag{10}$$

The result is:

$$[H_m^R]\{\delta_m\} + \sum_{n=1}^{\mu}[Q_{mn}]\{\delta_n\} = 0 \quad m = 1, 2, \ldots, \mu \tag{11}$$

where

$$[Q_{mn}] = \begin{vmatrix} c_{mn}[H_{11n}^I] - c_{nm}[H_{11m}^I] & c_{mn}[H_{12n}^I] - c_{nm}[H_{12m}^I] \\ c_{mn}[H_{21n}^I] - c_{nm}[H_{21m}^I] & c_{mn}[H_{22n}^I] - c_{nm}[H_{22m}^I] \end{vmatrix} \tag{12}$$

The matrices $[H_m^R]$ and $[Q_{mn}]$, and the vectors $\{\delta_m\}$, $\{\delta_n\}$, are real.

In Equation 11, when the shear stress τ is zero, Q_{mn} is zero and hence the individual series terms are uncoupled in m = 1, 2, ... , μ and each can be solved independently. Further, $[Q_{mn}]$ is the transpose of $[Q_{nm}]$ since $[H_m^I]$ is Hermitian so that the resulting stiffness and stability matrices are symmetric.

For example, when μ = 3 (3 series terms), the full stiffness and stability matrix derived from Equation 11 can be represented as follows:

$$[H] = \begin{bmatrix} [H_1^R] & [Q_{12}] & 0 \\ [Q_{21}] & [H_2^R] & [Q_{23}] \\ 0 & [Q_{32}] & [H_3^R] \end{bmatrix} = \begin{bmatrix} [H_1^R] & [Q_{12}] & 0 \\ [Q_{12}]^T & [H_2^R] & [Q_{23}] \\ 0 & [Q_{23}]^T & [H_3^R] \end{bmatrix} \tag{13}$$

The matrix [H] has 4 * N * μ degrees of freedom. If the rows and columns in the matrix [H] are organised so that each degree of freedom is taken over the μ series terms, then the half-bandwidth of the matrix is simply μ times the half-bandwidth of the problem with one series term. This speeds the computation of the eigenvalues and eigenvectors considerably.

ASSEMBLY OF STIFFNESS AND STABILITY MATRICES

The component flexural stiffness and stability matrices used to compute $[K_m]$ and $[G_m]$ in Eq. 5 (and hence $[H_m]$) was derived in Hancock and Pham (2011, 2012) to be:

$$([k_{Fm}] - \lambda_E[g_{Fm}])\{\delta_{Fm}\} = 0 \tag{14}$$

The flexural stiffness matrix $[k_{Fm}]$ is real and the flexural stability matrix $[g_{Fm}]$ is real if the shear stress τ is zero. However, the stability matrix $[g_{Fm}]$ is complex Hermitian if the shear stress is non-zero. They are given for the mth series term in Appendix C.

The component membrane stiffness and stability matrices used to compute $[K_m]$ and $[G_m]$ in Eq. 5 were derived by Hancock and Pham (2011, 2012) to be:

$$([k_{Mm}] - \lambda_E[g_{Mm}])\{\delta_{Mm}\} = 0 \tag{15}$$

The membrane stiffness matrix $[k_M]$ is real and the membrane stability matrix $[g_M]$ is real. They are given for the mth series term in Appendix D. The term λ_E is the load factor.

For folded plate assemblies including thin-walled sections such as channels, (14) and (15) must be transformed to a global co-ordinate system to assemble the stiffness $[K_m]$ and stability $[G_m]$ matrices of the folded plate assembly or section for the mth series term.

It is clear that only $[g_F]$ has complex terms. So only $[H_{11n}^{I}]$ and $[H_{11m}^{I}]$ in Equation 12 are non-zero. Equation 12 therefore simplifies to:

$$[Q_{mn}] = \begin{vmatrix} c_{mn}[H_{11n}^{I}] - c_{nm}[H_{11m}^{I}] & 0 \\ 0 & 0 \end{vmatrix} \quad (16)$$

EIGENVALUE ROUTINES

STURM SEQUENCE PROPERTY

From the theory of equations (Turnbull, 1946), the leading principal minors of [C]-λ[I] (where [I] is a unit matrix) form a Sturm sequence. The leading principal minor of order r is given by det ($[C_r]$ –λ[I]) where $[C_r]$ is the leading principal sub-matrix of order r of [C]. The first term of the Sturm sequence is the leading principal minor of order r=0 and is defined to be unity.

The number of eigenvalues greater than λ is equal to the number of agreements in sign between consecutive members of the Sturm sequence from r = 0 to r = n where n is the dimension of the matrix [C]. This property is very useful in isolating the range of λ in which a particular eigenvalue is located. The eigenvalue corresponding to a particular mode number can be isolated by bisection between values of λ which bound the eigenvalue.

DIRECT COMPUTATION OF SIGN COUNT OF ([A] - λ [B])

Peters and Wilkinson (1969) have shown that the sign of det($[A_r]$ – λ$[B_r]$) is the same as that of det($[C_r]$ – λ[I]). Consequently, it is possible to apply the Sturm sequence directly to ([A] - λ[B]) without the need to transform to the standard eigenvalue problem det([C] - λ[I]) = 0.

For the finite strip buckling analysis given by (11), the [G] component of [H] is chosen as [A] and the [K] component of [H] is chosen as [B] so that the computed eigenvalues λ of ([A] - λ[B]) are the reciprocals of the load factors λ_E

EIGENVECTOR CALCULATION

Wilkinson (1958) has produced a method for computing the eigenvector {δ} of (11) by solving the equations at the value of λ_E for a unit right hand side vector {1} replacing {0} in (11). The process is usually repeated once to purify the eigenvector with the unit vector {1} replaced by {δ} from the first iteration. This method has been used in the calculations in this report.

COMPUTER PROGRAM bfinst8.cpp

A computer program **bfinst8.cpp** has been written in Visual Studio C++ to assemble the stiffness and stability matrices given by Equation 11 and to solve for the eigenvalues using the Sturm sequence property described in the Sections above, and to compute the corresponding eigenvectors as per the Section above. The program stores the real [K] matrix and the real [G] and complex [GI] components of the stability matrices in order to extract the eigenvalues and eigenvectors. The results from this analysis are given the notation reSAFSM (restrained SAFSM) in this report to distinguish it from the unrestrained SAFSM in Hancock and Pham (2011, 2012).

SOLUTIONS TO PLATES AND SECTIONS IN SHEAR

PLATE SIMPLY SUPPORTED ON BOTH LONGITUDINAL EDGES

The solution for a plate simply supported along both longitudinal edges determined using the reSAFSM analysis is compared with the classical solution of Timoshenko and Gere (1961) Item 9.7 Buckling of rectangular plates under the action of shearing stresses. The equation for the elastic buckling of a rectangular plate is given (Timoshenko and Gere (1961)) as:

$$\tau_{cr} = \frac{k_v \pi^2 D}{t\, b^2} \qquad (17)$$

where D is the plate flexural rigidity, b is the width of the plate which may consist of multiple strips and k_v is the plate buckling coefficient in shear.

The analysis is carried out for 8 equal width strips and an increasing number of series terms. Aspect ratios of 1:1, 2:1, 3:1 and 4:1 have been investigated and the solutions for the buckling coefficient k_v are compared in Table 1 with those of Timoshenko and Gere Table 9-10. It is clear that the solutions become more accurate with increasing numbers of series terms, and that more terms are required for higher aspect ratios. The solutions converge to values slightly lower than those of Timoshenko and Gere (1961) presumably because they used less series terms. These k_v values can be compared with that for a buckle in an infinitely long section of 5.3385 given in Plank and Wittrick (1974) and Hancock and Pham (2011, 2012). Anderson and Williams (1985) achieved values of 9.37, 9.35 and 9.32 for 6 strips and 3, 4 and 6 series terms respectively using the exact strip formulation for a square plate simply supported along all four longitudinal edges.

Aspect ratio	Timoshenko and Gere (1961)	3 series terms	4 series terms	6 series terms
1:1	9.34	9.379	9.366	9.332
2:1	6.6	6.691	6.564	6.551
3:1	5.9	6.644	5.898	5.849
4:1	5.7	7.219	6.029	5.645

Table 1 Buckling coefficients k_v for simply supported square and rectangular plates

The buckling modes for an aspect ratio of 2:1 and 6 series terms determined from bfinst8.cpp are plotted as a contour plot using Mathcad in Fig. 3. The buckling mode has one elongated local buckle of the web satisfying the simply supported boundary conditions on all four edges. The contour line finishing at the centres of the ends is the zero displacement contour.

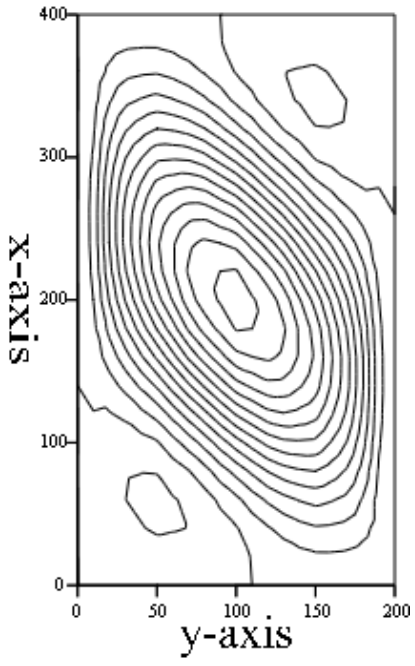

Figure 3. Shear Buckling Mode of Plate of Aspect Ratio 2:1
with Four Edges Simply Supported (6 Series Terms)

LIPPED CHANNEL SECTION IN PURE SHEAR

In order to extend the study to lipped channel sections, a 200mm deep lipped channel with flange width 80mm, lip length 20mm and thickness 2mm as studied by Pham and Hancock (2009a, 2012b) has been used. These dimensions are all centreline and not overall. In Pham and Hancock (2009a), three different shear stress distributions have been investigated. These are uniform shear in the web alone (called Cases A/B), uniform shear in the web and flanges (called Case C), and a shear stress equivalent to a shear flow as occurs in a channel section under a shear force parallel with the web through the shear centre (Case D as shown in Fig. 4). In this report, only Case D is studied as it is the most representative of practice. The shear flow distribution is not in equilibrium longitudinally as this can only be achieved by way of a moment gradient in the section. However, it has been used in these studies to isolate the shear from the bending for the purpose of identifying pure shear buckling loads and modes. The finite strip buckling analysis allows the uniform shear stresses in each strip, as shown in Fig. 2, to be used to assemble the stability matrix $[\underline{k}_g]$ of each strip then the system stability matrix [G]. Fig. 4 demonstrates that the shear flow in each strip is uniform. In the studies of plain channels in this report, the web is divided into sixteen equal width strips, the flanges into ten each and the lips into two each making 40 strips and 41 nodal line with a total of 164 degrees of freedom. Adequate accuracy can be achieved for engineering purposes with 18 strips, 19 nodal lines and 76 degrees of freedom. However, 40 strips have been used in this case for accurate benchmarking against the SFSM analyses.

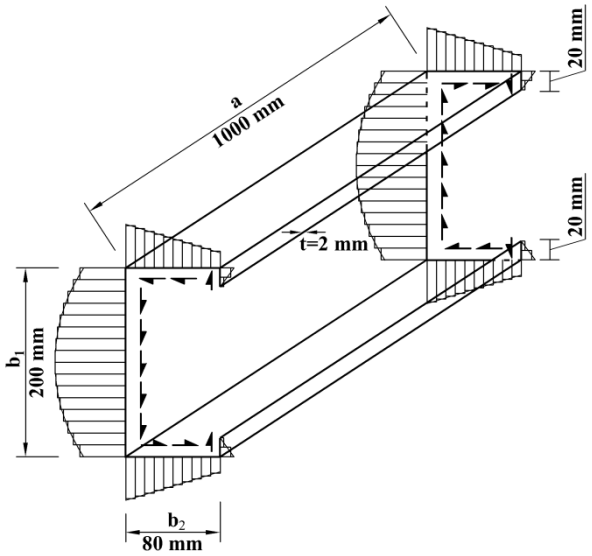

Figure 4. Shear Flow Distribution Assumed (Case D)

The SAFSM and reSAFSM curves of buckling stress versus half-wavelength/length are compared in Fig. 5. The reSAFSM graph (circles) of buckling stress versus length (as opposed to half-wavelength for the SAFSM) was computed using the **bfinst8.cpp** program described above with 8 series terms. The reSAFSM analysis assumes no cross-section distortion at both ends of the section under analysis (Z = 0, L). For a section of length 200mm, the reSAFSM analysis gives a buckling coefficient k_v of 10.017 for the web which is higher than that for a square panel in shear at 9.34 due to the flange restraint. The buckling mode is shown in Fig. 6 and encompasses a single buckle half-wavelength. At L = 600mm, 1000mm and 1600mm, the buckling modes are shown in Fig. 7, 8 and 9 respectively and involve 3, 5 and 6 local buckle half-waves respectively. At L = 2000mm, the buckling mode involves one half-wavelength and is a type of distortional buckle and is shown in Fig. 10.

For comparison, the SAFSM graph (squares) of buckling stress versus buckle half-wavelength (signature curve) derived in Hancock and Pham (2011, 2012) using the program **bfinst7.cpp** is also shown in Fig. 5 for the lipped channel for a range of buckle half-wavelengths from 30mm to 10000mm. The graph reaches a minimum at approximately 200mm half-wavelength then rises and starts to drop at about 800mm. The buckling coefficient k_v corresponding to the minimum point is 6.583 based on the average stress in the web ($\tau_{av} = V/A_w$) computed from the shear load V on the section divided by the area of the web A_w. This compares with an asymptotic value of 6.60 for multiple local buckles using the reSAFSM analysis.

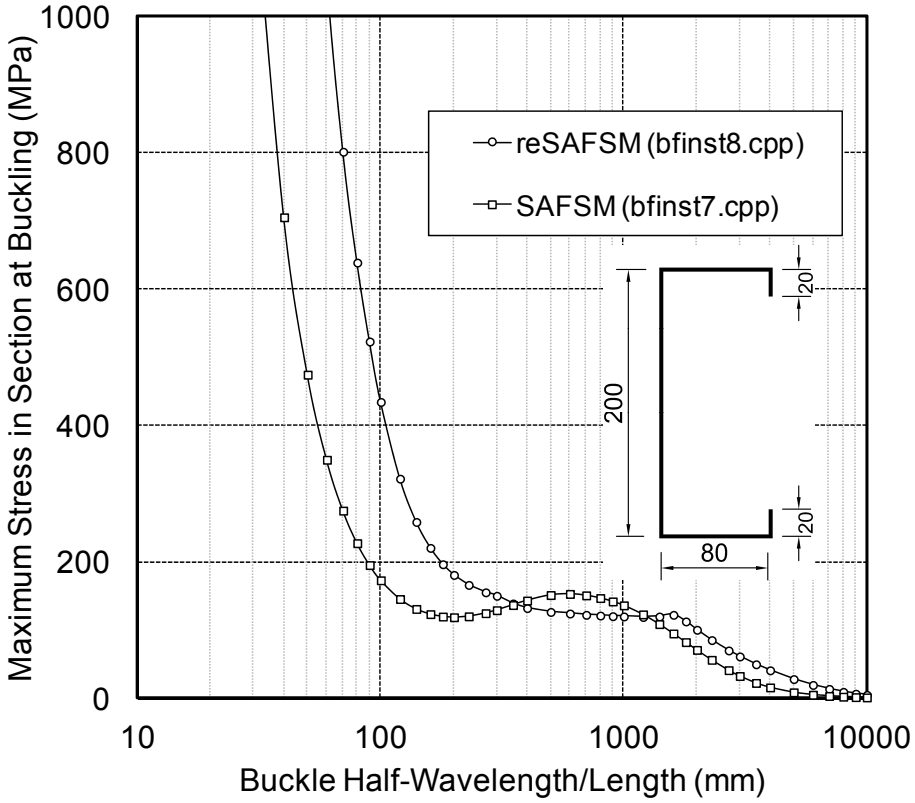

Figure 5. Buckling Stress versus Length/Half-Wavelength from SAFSM (bfinst7.cpp) and reSAFSM (bfinst8.cpp) for Simple Lipped Channel

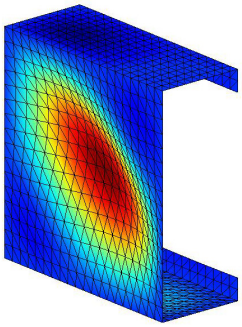

Figure 6. Simple Lipped Channel Shear Buckling Mode at L = 200mm

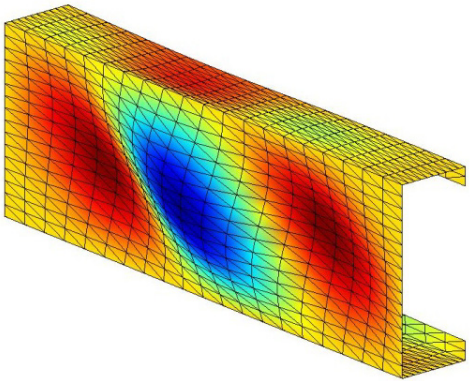

Figure 7. Simple Lipped Channel Shear Buckling Mode at L = 600mm

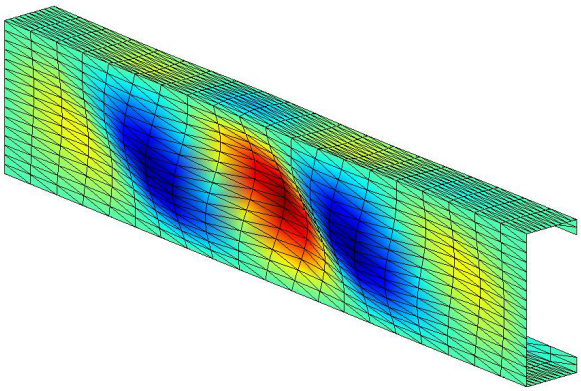

Figure 8. Simple Lipped Channel Shear Buckling Mode at L = 1000mm

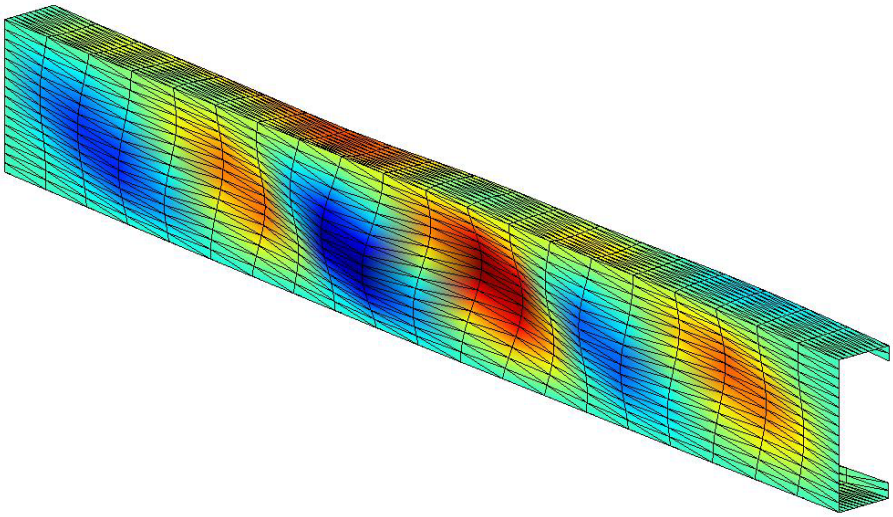

Figure 9. Simple Lipped Channel Shear Buckling Mode at L = 1600mm

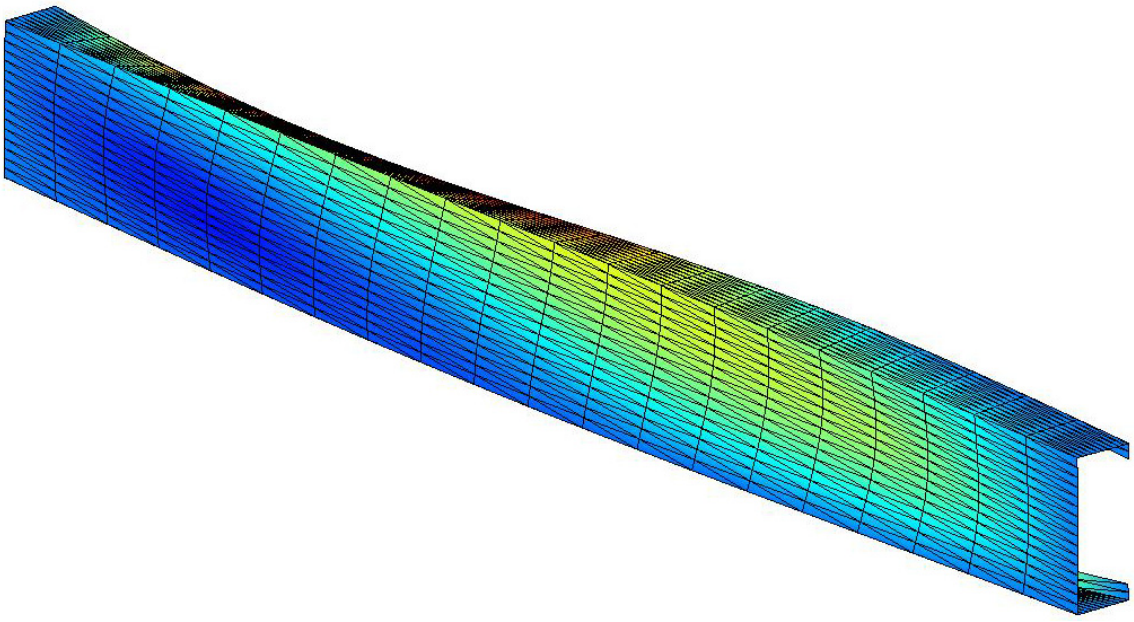

Figure 10. Simple Lipped Channel Shear Buckling Mode at L = 2000mm

To validate the accuracy of the reSAFSM analysis, the buckling stresses and coefficients are compared in Appendix A with the Spline Finite Strip Method (SFSM) reported in Pham and Hancock (2009a, 2012b). The SFSM values have also been computed for a section with the same strip subdivision of 40 strips and can be regarded as an accurate solution for benchmarking. They were given previously in Hancock and Pham (2011, 2012). In general, the reSAFSM values are higher than the SFSM values by less than 1%. However, at L=1600mm, the error increases to approximately 4% as the use of only 8 series terms does not accurately predict the behaviour when at least 6 buckle half-waves occur as shown in Fig. 9.

WEB-STIFFENED CHANNEL IN PURE SHEAR

Shear buckling of thin-walled channel sections with intermediate web stiffeners have been studied using the SFSM by Pham and Hancock (2009b) and using the SAFSM by Hancock and Pham (2011, 2012) and Pham SH, Pham CH and Hancock (2012a, 2012b). In this report, the particular web stiffener used is the same as that in Hancock and Pham (2011, 2012) and has a rectangular indent of 5mm over a depth of 80mm located symmetrically about the centre of the web. Swage stiffeners of this type are common in practice. The web is divided into 6 equal width strips for each of the 2 outer vertical elements in the web, 8 for the inner vertical element of the web, the stiffeners in the web into 2 each, the flanges into 6 each and the lips into two each making 40 strips and 41 nodal line with a total of 164 degrees of freedom, the same number as for the simple lipped channel.

The SAFSM and reSFSM curves of buckling stress versus half-wavelength/length are compared in Fig.11. The effect of the different end conditions (Z = 0,L) between the SAFSM (squares) and reSAFSM (circles) are clear from this comparison. The shape of the two curves is remarkably similar except that the SFSM shows several plateau points at approximately 200mm and 1000mm lengths corresponding to the switch in buckling modes. The differences in the modes at these switch points are shown in Figs. 12, 13 and 14.

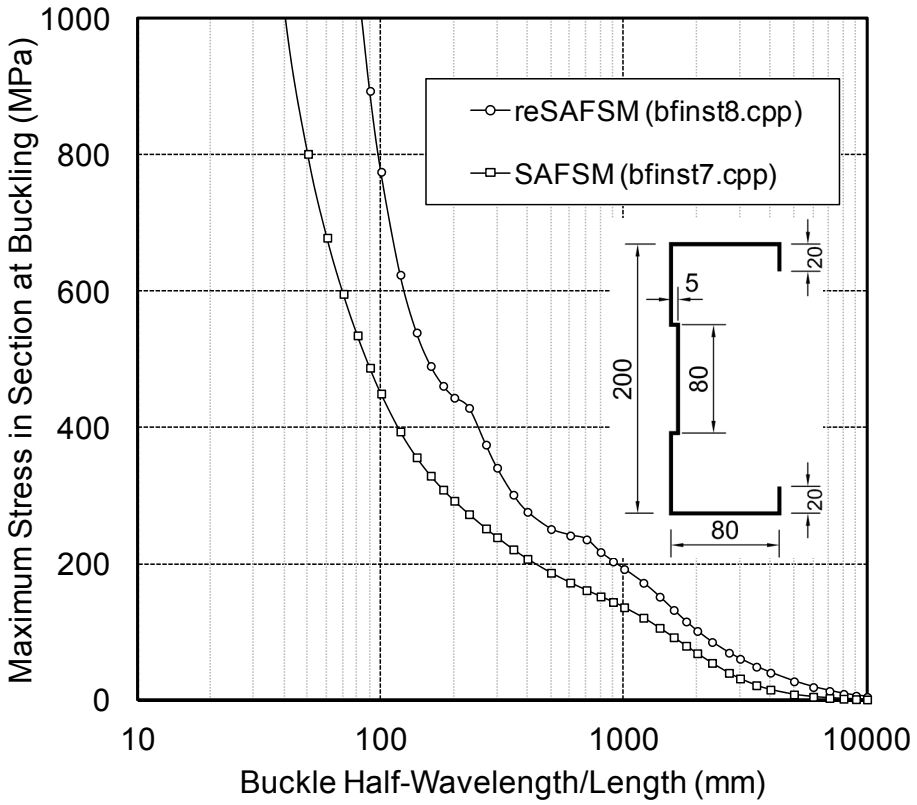

Figure 11. Buckling Stress versus Length/Half-Wavelength from SAFSM (bfinst7.cpp) and reSAFSM (bfinst8.cpp) for Stiffened web Channel

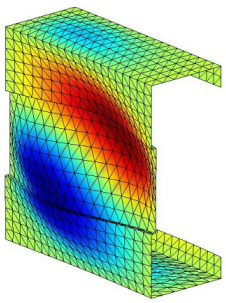

Figure 12. Stiffened web channel shear buckling mode at L = 200mm

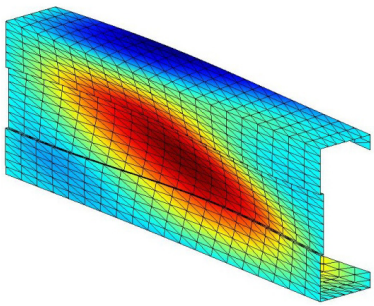

Figure 13. Stiffened web channel shear buckling mode at L = 600mm

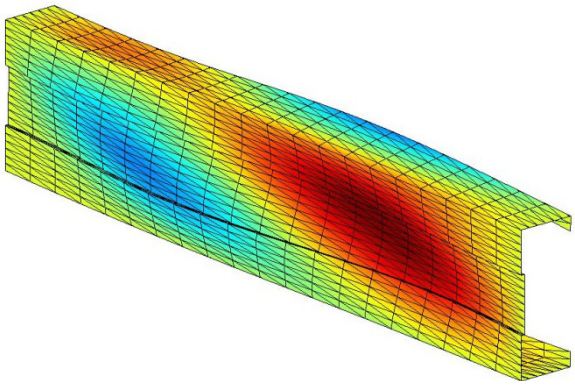

Figure 14. Stiffened web channel shear buckling mode at L = 1000mm

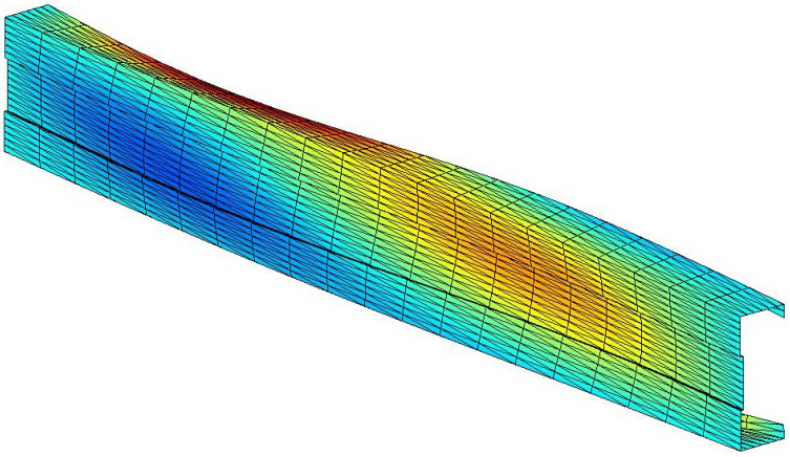

Figure 15. Stiffened web channel shear buckling mode at L = 1600mm

It is interesting to observe that the stiffened web channel has only two buckle half-waves at a length of 1000mm compared with five for the plain channel. The effect of the stiffener is to decrease the number of buckle half-waves with a corresponding increase in the buckling stress.

To validate the accuracy of the reSAFSM analysis for the web stiffened channel, the buckling stresses and coefficients are compared in Appendix B with the Spline Finite Strip Method (SFSM) reported in Hancock and Pham (2011). The SFSM values have also been computed for a section with 40 strips and can be regarded as an accurate solution for benchmarking. In general, the reSAFSM values are higher than the SFSM values by less than 1% for lengths greater than 600mm. At shorter lengths, the error is slightly higher decreasing from 3.8% at 100mm to 1.8% at 200mm for the mode shown in Fig. 12 then falling rapidly to 0.5% at 400mm.

CONCLUSIONS

A new version of the semi-analytical finite strip buckling analysis of thin-flat-walled structures under combined loading with simply supported end conditions has been derived and programmed in Visual Studio C++. The method has been called reSAFSM to reflect the restrained ends. The method uses multiple series terms to allow for the increasing numbers of buckle half-waves as the sections become longer. The method includes the extraction of the eigenvalues and eigenvectors from the matrices produced when thin-walled sections are subjected to shear in addition to compression and bending. The method is based on the theory of Anderson and Williams applied to the general complex matrices developed by Plank and Wittrick. The method using up to 6 series terms has been checked against the solutions of Timoshenko and Gere for simply supported rectangular plate in pure shear and found to produce accurate results. The solutions are slightly more accurate than Timoshenko and Gere as more series terms have been used.

The buckling stress versus length curve for a plain lipped channel in pure shear has been produced using the reSAFSM with 8 series terms and compared with the signature curve from semi-analytical finte strip method with unrestrained ends (SAFSM). The reSFSM curve has also been compared with the spline finite strip buckling analysis (SFSM) where the ends are fixed against distortion. For the subdivision of the section into 40 strips, the method is accurate to generally better than 1% except in the at L=1600mm where an error of 4% occurs and more series terms would be required at this length before the mode switches to a single distortional buckle at longer half-wavelengths.

The buckling stress versus length for a web-stiffened lipped channel with a 5mm swage stiffener has also been investigated. The modes have changed significantly from those of the simple lipped channel. Accuracies generally better than 1% have been achieved compared with the SFSM analysis except at lengths less than 200mm where an error of 1.8% occurs**.**

ACKNOWLEDGEMENTS

Funding provided by the Australian Research Council Discovery Project Grant DP110103948 has been used to perform this project. The SFSM program used was developed by Gabriele Eccher. The graphics program used to draw the 3D buckling modes was developed by Song Hong Pham under an Australian Government AusAid Scholarship.

REFERENCES

Adany, S. and Schafer, B.W. (2006), “Buckling mode decomposition of thin-walled, single branched open cross-section members via a constrained finite strip method”, Thin-Walled Structures, 64(1): p 12.29.

Anderson, M.S. and Williams, F.W. (1985), “Buckling of simply supported plate assemblies subject to shear loading”, Aspects of the analysis of plate structures, (Eds. Dawe et al), Clarendon Press, Oxford, pp 39-50.

American Iron and Steel Institute (AISI). (2007). "North American Specification for the Design of Cold-Formed Steel Structural Members." 2007 Edition, AISI S100-2007.

Centre for Advanced Structural Engineering (2006), "THIN-WALL – A computer program for cross-section analysis and finite strip buckling analysis and direct strength design of thin-walled structures", Version 2.1, School of Civil Engineering, the University of Sydney, Sydney, Australia.

Cheung, Y. K. (1968) "Finite Strip Method Analysis of Elastic Slabs." *ASCE J. Eng. Mech. Div.*, Vol. 94, EM6, pp. 1365-1378.

Cheung, Y.K. (1976), Finite Strip Method in Structural Analysis, Pergamon Press, Inc. New York, N.Y.

Hancock, G. J. and Pham, C. H. (2011), "A Signature Curve for Cold-Formed Channel Sections in Pure Shear", Research Report R919, School of Civil Engineering, the University of Sydney, July.

Hancock, G. J. and Pham, C. H. (2012), "Direct Method of Design for Shear of Cold-Formed Channel Sections based on a Shear Signature Curve ", Proceedings, 21st International Specialty Conference on Cold-Formed Steel Structures (Eds. LaBoube and Yu), St Louis, Missouri, USA, Oct , pp 207 – 221.

Lau, S. C. W. and Hancock, G. J. (1986). "Buckling of Thin Flat-Walled Structures by a Spline Finite Strip Method." Thin-Walled Structures, Vol. 4, pp 269-294.

Peters, G. and Wilkinson, J.H. (1969), "Eigenvalues of Ax = λBx with Band Symmetric A and B", Computer Journal, Vol. 12, pp 398-404.

Pham, C. H. and Hancock, G. J. (2009a). "Shear Buckling of Thin-Walled Channel Sections." Journal of Constructional Steel Research, Vol. 65, No. 3, pp. 578-585.

Pham, C. H. and Hancock, G. J. (2009b). "Shear Buckling of Thin-Walled Channel Sections with Intermediate Web Stiffener." Proceedings, Sixth International Conference on Advances in Steel Structures, Hong Kong, pp. 417-424.

Pham, C. H. and Hancock, G. J. (2012a). "Direct Strength Design of Cold-Formed C-Sections for Shear and Combined Actions" Journal of Structural Engineering, ASCE, Vol. 138, No. 6, pp 759-768.

Pham, C. H. and Hancock, G. J. (2012b) "Elastic Buckling of Cold-Formed Channel Sections in Shear." Thin-Walled Structures, Vol. 61, pp. 22-26.

Pham, S.H., Pham, C.H. and Hancock, G.J. (2012a), "Shear Buckling of Thin-Walled Channel Sections with Complex Stiffened Webs", Research Report R924, School of Civil Engineering, the University of Sydney, January.

Pham, S.H., Pham, C.H. and Hancock, G.J.(2012b), "Shear Buckling of Thin-Walled Channel Sections with Complex Stiffened Webs", Proceedings, 21st International Specialty Conference on Cold-Formed Steel Structures (Eds. LaBoube and Yu), St Louis, Missouri, USA, Oct 2012, pp 281-296.

Plank, RJ and Wittrick, WH. (1974), "Buckling Under Combined Loading of Thin, Flat-Walled Structures by a Complex Finite Strip Method", International Journal for Numerical Methods in Engineering, Vol. 8, No. 2, pp 323-329.

Standards Australia. (2005). "AS/NZS 4600:2005, Cold-Formed Steel Structures." Standards Australia/ Standards New Zealand.

Timoshenko, S.P. and Gere, JM. (1961),"Theory of Elastic Stability", McGraw-Hill Book Co. Inc., New York, N.Y.

Turnbull, H.W. (1946), Theory of Equations, Oliver and Boyd, Edinburgh and London.

Wilkinson, J.H. (1958), "The calculation of the eigenvectors of co-diagonal matrices", Computer Journal, Vol. 1, pp 90-96.

Williams, F.W. and Wittrick, W.H. (1969), "Computational procedures for a matrix analysis f the stability and vibration of thin flat-walled structures in compression", Int. Journal of Mechanical Sciences, 11, 979-998.

Wittrick, W.H. (1968), "A unified approach to the initial buckling of stiffened panels in compression", Aeronautical Quarterly, 19, 265-283.

APPENDIX A: BUCKLING STRESS AND SHEAR BUCKLING COEFFICIENT FOR PLAIN LIPPED CHANNEL

Table A. Buckling Stress and Buckling Coefficient for Plain Lipped Channel

Length (mm)	reSAFSM (8 terms)		SFSM	
	Buckling Stress (MPa)	Shear Buckling Coefficient k_v	Buckling Stress (MPa)	Shear Buckling Coefficient k_v
30	3973.952	219.847	3735.470	206.651
40	2281.488	126.216	2188.912	121.094
50	1493.687	82.834	1451.298	80.288
60	1062.087	58.757	1039.176	57.489
70	801.930	44.364	786.997	43.538
80	639.272	35.366	628.730	34.782
90	523.503	28.961	516.653	28.582
100	434.828	24.056	429.473	23.759
120	322.269	17.829	318.626	17.627
140	258.758	14.315	256.026	14.164
160	220.704	12.210	218.510	12.088
180	196.747	10.884	194.899	10.782
200	181.059	10.017	179.450	9.927
230	166.424	9.207	165.063	9.132
270	155.543	8.605	154.413	8.542
300	150.447	8.323	149.455	8.268
350	139.202	7.701	138.477	7.661
400	132.450	7.327	131.794	7.291
500	126.762	7.013	126.202	6.982
600	124.451	6.885	123.833	6.851
700	122.526	6.778	121.996	6.749
800	121.494	6.721	120.920	6.689
900	120.552	6.669	119.980	6.637
1000	120.165	6.648	119.440	6.608
1200	119.323	6.601	118.620	6.562
1400	120.070	6.642	118.111	6.534
1600	122.499	6.777	117.770	6.515
1800	112.839	6.242	111.764	6.183
2000	100.604	5.566	99.588	5.509
2300	85.460	4.728	84.609	4.681
2700	70.262	3.887	69.605	3.851
3000	61.466	3.400	60.914	3.370
3500	49.989	2.765	49.561	2.742
4000	41.132	2.276	40.795	2.257
5000	28.260	1.563	28.049	1.552
6000	19.666	1.088	19.536	1.081
7000	13.830	0.765	13.786	0.763
8000	9.512	0.526	9.484	0.525
9000	6.823	0.377	6.805	0.376
10000	5.059	0.280	5.056	0.280

APPENDIX B: BUCKLING STRESS AND SHEAR BUCKLING COEFFICIENT FOR STIFFENED WEB CHANNEL

Table **B**. Buckling Stress and Buckling Coefficient for Stiffened Web Channel

Half-Wavelength/ Length (mm)	reSAFSM (8 terms)		SFSM	
	Buckling Stress (MPa)	Shear Buckling Coefficient k_v	Buckling Stress (MPa)	Shear Buckling Coefficient k_v
30	4255.165	235.404	3963.104	219.244
40	2583.108	142.902	2469.557	136.619
50	1804.562	99.832	1737.175	96.103
60	1422.517	78.696	1374.149	76.020
70	1212.321	67.068	1173.947	64.944
80	1058.671	58.568	1033.547	57.177
90	894.272	49.473	874.267	48.366
100	775.562	42.906	758.890	41.983
120	624.469	34.547	611.755	33.843
140	539.751	29.860	529.189	29.275
160	490.584	27.140	481.298	26.626
180	461.497	25.531	453.027	25.062
200	444.027	24.564	436.119	24.127
230	429.122	23.740	421.860	23.338
270	375.225	20.758	369.918	20.464
300	341.310	18.882	336.908	18.638
350	301.747	16.693	298.380	16.507
400	276.622	15.303	273.891	15.152
500	251.326	13.904	249.221	13.787
600	241.917	13.383	240.095	13.282
700	236.144	13.064	234.431	12.969
800	217.576	12.037	216.227	11.962
900	203.801	11.275	202.662	11.212
1000	192.627	10.657	191.610	10.600
1200	172.487	9.542	171.589	9.493
1400	152.111	8.415	151.281	8.369
1600	132.635	7.338	131.884	7.296
1800	115.757	6.404	115.098	6.367
2000	101.839	5.634	101.267	5.602
2300	85.587	4.735	85.120	4.709
2700	69.865	3.865	69.493	3.844
3000	60.935	3.371	60.610	3.353
3500	49.419	2.734	49.148	2.719
4000	40.618	2.247	40.386	2.234
5000	27.918	1.544	27.747	1.535
6000	19.464	1.077	19.339	1.070
7000	13.751	0.761	13.706	0.758
8000	9.461	0.523	9.430	0.522
9000	6.788	0.376	6.766	0.374
10000	5.044	0.279	5.027	0.278

APPENDIX C: FLEXURAL STIFFNESS AND STABILITY MATRICES FOR MTH SERIES TERM

$$[k_{Fm}] = [C_F]^{-T}\,[k_{\alpha Fm}]\,[C_F]^{-1} \tag{C-1}$$

$$[g_{Fm}] = [C_F]^{-T}\,[g_{\alpha Fm} + i g_{\alpha Sm}]\,[C_F]^{-1} \tag{C-2}$$

where

$$[C_F]^{-1} = \begin{bmatrix} 1 & 0 & 0 & 0 \\ 0 & b & 0 & 0 \\ -3 & -2b & 3 & -b \\ 2 & b & -2 & b \end{bmatrix}$$

$[k_{\alpha Fm}]$ =

$$\begin{bmatrix} \left(\frac{DX}{2}\right) & \left(\frac{DX}{4}\right) & \left(\frac{DX}{6} - D1\right) & \left(\frac{DX}{8} - \frac{3D1}{2}\right) \\ \left(\frac{DX}{4}\right) & \left(\frac{DX}{6} + 2DXY\right) & \left(\frac{DX}{8} - \frac{D1}{2} + 2DXY\right) & \left(\frac{DX}{10} - D1 + 2DXY\right) \\ \left(\frac{DX}{6} - D1\right) & \left(\frac{DX}{8} - \frac{D1}{2} + 2DXY\right) & \left(\frac{DX}{10} - \frac{2D1}{3} + 2DY + \frac{8DXY}{3}\right) & \left(\frac{DX}{12} - D1 + 3DY + 3DXY\right) \\ \left(\frac{DX}{8} - \frac{3D1}{2}\right) & \left(\frac{DX}{10} - D1 + 2DXY\right) & \left(\frac{DX}{12} - D1 + 3DY + 3DXY\right) & \left(\frac{DX}{14} - \frac{6D1}{5} + 6DY + \frac{18DXY}{5}\right) \end{bmatrix}$$

where

$$DX = D\left(\frac{m\pi}{L}\right)^4 A$$

$$DY = \frac{D}{b^4} A$$

$$D1 = \nu D \left(\frac{m\pi}{bL}\right)^2 A$$

$$DXY = \frac{G t^3}{12}\left(\frac{m\pi}{bL}\right)^2 A$$

$$A = b L$$

$$D = \frac{E t^3}{12 (1 - \nu^2)}$$

$$[g_{\alpha Fm}] = \begin{bmatrix} \left(f_1 + \frac{f_2}{2}\right) & \left(\frac{f_1}{2} + \frac{f_2}{3}\right) & \left(\frac{f_1}{3} + \frac{f_2}{4}\right) & \left(\frac{f_1}{4} + \frac{f_2}{5}\right) \\ \left(\frac{f_1}{2} + \frac{f_2}{3}\right) & \left(\frac{f_1}{3} + \frac{f_2}{4} + f_3\right) & \left(\frac{f_1}{4} + \frac{f_2}{5} + f_3\right) & \left(\frac{f_1}{5} + \frac{f_2}{6} + f_3\right) \\ \left(\frac{f_1}{3} + \frac{f_2}{4}\right) & \left(\frac{f_1}{4} + \frac{f_2}{5} + f_3\right) & \left(\frac{f_1}{5} + \frac{f_2}{6} + \frac{4f_3}{3}\right) & \left(\frac{f_1}{6} + \frac{f_2}{7} + \frac{6f_3}{4}\right) \\ \left(\frac{f_1}{4} + \frac{f_2}{5}\right) & \left(\frac{f_1}{5} + \frac{f_2}{6} + f_3\right) & \left(\frac{f_1}{6} + \frac{f_2}{7} + \frac{6f_3}{4}\right) & \left(\frac{f_1}{7} + \frac{f_2}{8} + \frac{9f_3}{5}\right) \end{bmatrix}$$

where

$$f_1 = \left(\frac{m\pi}{L}\right)^2 \frac{V}{2} \sigma_1$$

$$f_2 = \left(\frac{m\pi}{L}\right)^2 \frac{V}{2} (\sigma_2 - \sigma_1)$$

$$f_3 = \left(\frac{1}{b}\right)^2 \frac{V}{2} \sigma_T$$

$$V = b\,t\,L$$

$$[g_{\alpha Sm}] = \begin{bmatrix} 0 & f_4 & f_4 & f_4 \\ -f_4 & 0 & \frac{f_4}{3} & \frac{f_4}{2} \\ -f_4 & -\frac{f_4}{3} & 0 & \frac{f_4}{5} \\ -f_4 & -\frac{f_4}{2} & -\frac{f_4}{5} & 0 \end{bmatrix}$$

$$f_4 = \left(\frac{m\pi}{bL}\right) \frac{V}{2} \tau$$

The stresses σ_1, σ_2, σ_T and τ are shown in Fig. 2

APPENDIX D: MEMBRANE STIFFNESS AND STABILITY MATRICES FOR MTH SERIES TERM

$$[k_{Mm}] = [C_M]^{-T}\,[k_{\alpha Mm}]\,[C_M]^{-1} \tag{D-1}$$

$$[g_{Mm}] = [C_M]^{-T}\,[g_{\alpha Mm}]\,[C_M]^{-1} \tag{D-2}$$

where

$$[C_M]^{-1} = \begin{bmatrix} 1 & 0 & 0 & 0 \\ -1 & 0 & 1 & 0 \\ 0 & 1 & 0 & 0 \\ 0 & -1 & 0 & 1 \end{bmatrix}$$

$[k_{\alpha Mm}]$ =

$$\begin{bmatrix} \left(\frac{G1}{2}\right) & \left(\frac{G1}{4}\right) & 0 & \left(\frac{G1}{2bk}\right) \\ \left(\frac{G1}{4}\right) & \left(\frac{G1}{6}+\frac{E1}{2}\right) & \left(\frac{-E12}{2}\right) & \left(\frac{G1}{4bk}-\frac{E12}{4}\right) \\ 0 & \left(\frac{-E12}{2}\right) & \left(\frac{E2}{2}\right) & \left(\frac{E2}{4}\right) \\ \left(\frac{G1}{2bk}\right) & \left(\frac{G1}{4bk}-\frac{E12}{4}\right) & \left(\frac{E2}{4}\right) & \left(\frac{G1}{2(bk)^2}+\frac{E2}{6}\right) \end{bmatrix}$$

where

$$G1 = G\left(\frac{m\pi}{L}\right)^2 V$$
$$E1 = \frac{E_1}{b^2}\,V$$
$$E2 = E_1\left(\frac{m\pi}{L}\right)^2 V$$
$$E12 = \nu E_1\left(\frac{m\pi}{bL}\right)V$$
$$V = b\,t\,L$$
$$k = \frac{m\pi}{L}$$
$$E_1 = \frac{E}{(1-\nu^2)}$$

$$[g_{\alpha Mm}] = \begin{bmatrix} \left(f_1+\frac{f_2}{2}\right) & \left(\frac{f_1}{2}+\frac{f_2}{3}\right) & 0 & 0 \\ \left(\frac{f_1}{2}+\frac{f_2}{3}\right) & \left(\frac{f_1}{3}+\frac{f_2}{4}\right) & 0 & 0 \\ 0 & 0 & \left(f_1+\frac{f_2}{2}\right) & \left(\frac{f_1}{2}+\frac{f_2}{3}\right) \\ 0 & 0 & \left(\frac{f_1}{2}+\frac{f_2}{3}\right) & \left(\frac{f_1}{3}+\frac{f_2}{4}\right) \end{bmatrix}$$

where

$$f_1 = \left(\frac{m\pi}{L}\right)^2 \frac{V}{2}\,\sigma_1$$
$$f_2 = \left(\frac{m\pi}{L}\right)^2 \frac{V}{2}\,(\sigma_2 - \sigma_1)$$
$$V = b\,t\,L$$